Carcinogenesis vol.22 no.1 pp.115–125, 2001

Neoplastic transformation of human osteoblast cells to the tumorigenic phenotype by heavy metal–tungsten alloy particles: induction of genotoxic effects

Alexandra C.Miller[3] Steve Mog[1], LuAnn McKinney[1], Lei Luo[2], Jennifer Allen, Jiaquan Xu and Natalie Page[2]

Applied Cellular Radiobiology Department and [1]Veterinary Sciences Department, Armed Forces Radiobiology Research Institute, Bethesda, MD 20889-5603 and [2]Molecular Oncology Branch, Division of Cancer Treatment, National Cancer Institute, National Institutes of Health, Bethesda, MD 20892, USA

[3]To whom correspondence should be addressed at: AFRRI, Applied Cellular Radiobiology Department, 8901 Wisconsin Avenue, Bethesda, MD 20889-5603, USA

Heavy metal–tungsten alloys (HMTAs) are dense heavy metal composite materials used primarily in military applications. HMTAs are composed of a mixture of tungsten (91–93%), nickel (3–5%) and either cobalt (2–4%) or iron (2–4%) particles. Like the heavy metal depleted uranium (DU), the use of HMTAs in military munitions could result in their internalization in humans. Limited data exist, however, regarding the long-term health effects of internalized HMTAs in humans. We used an immortalized, non-tumorigenic, human osteoblast-like cell line (HOS) to study the tumorigenic transforming potential of reconstituted mixtures of tungsten, nickel and cobalt (rWNiCo) and tungsten, nickel and iron (rWNiFe). We report the ability of rWNiCo and rWNiFe to transform immortalized HOS cells to the tumorigenic phenotype. These HMTA transformants are characterized by anchorage-independent growth, tumor formation in nude mice and high level expression of the K-*ras* oncogene. Cellular exposure to rWNiCo and rWNiFe resulted in 8.90 ± 0.93- and 9.50 ± 0.91-fold increases in transformation frequency, respectively, compared with the frequency in untreated cells. In comparison, an equivalent dose of crystalline NiS resulted in a 7.7 ± 0.73-fold increase in transformation frequency. The inert metal tantalum oxide did not enhance HOS transformation frequency above untreated levels. The mechanism by which rWNiCo and rWNiFe induce cell transformation *in vitro* appears to involve, at least partially, direct damage to the genetic material, manifested as increased DNA breakage or chromosomal aberrations (i.e. micronuclei). This is the first report showing that HMTA mixtures of W, Ni and Co or Fe cause human cell transformation to the neoplastic phenotype. While additional studies are needed to determine if protracted HMTA exposure produces tumors *in vivo*, the implication from these *in vitro* results is that the risk of cancer induction from internalized HMTAs exposure may be comparable with the risk from other biologically reactive and insoluble carcinogenic heavy metal compounds (e.g. nickel subsulfide and nickel oxide).

Abbreviations: ALP, alkaline phosphatase; DU, depleted uranium; HMTA, heavy metal–tungsten alloys; HOS, human osteosarcoma; MN, micronuclei; MN-CB, micronucleated cytokinesis-blocked; ROS, reactive oxygen species.

Introduction

Heavy metals such as depleted uranium (DU) and tungsten are used as kinetic energy penetrators in military applications. While the use of DU in these applications has been limited to the USA, heavy metal–tungsten alloy (HMTA) penetrators (tungsten/nickel/iron and tungsten/nickel/cobalt) are manufactured and have been tested in numerous countries and are deployed world wide. A friendly fire accident that occurred during the Gulf War, resulting in US soldiers with retained large DU fragments (~2–20 mm), has focused attention on the potential health effects of internalized heavy metals like tungsten and DU used in military applications.

Several recent studies have investigated the potential health effects of militarily relevant heavy metals (1–5). These investigations have not only demonstrated the transforming ability (1) and mutagenicity (2) of DU, but also its neurotoxicity (5). In contrast, there is no information regarding the health effects of imbedded HMTAs. Studies have shown that occupational exposure to hard metal dust, a mixture of cobalt- and tungsten carbide-containing particles, is associated with development of different pulmonary diseases, including fibrosing alveolitis and lung cancer (6,7). The toxic properties of hard metal particles are not only attributed to an interaction between cobalt metal and carbide particles (8), but also to the production of hydroxyl radicals, which have been implicated in their genotoxic effects (9). The HMTAs used in military applications, however, are somewhat different from conventional hard metal. HMTA penetrators consist of a combination of tungsten, nickel and either cobalt or iron (tungsten >90%, nickel 1–6%, iron 1–6% or cobalt ~1–6%), in contrast to hard metal dust, which is a mixture of cobalt metal (5–10%) and tungsten carbide particles (>80%) (10). The differences in metal composition and percentages of hard metal particles and tungsten alloys used in military applications preclude the assumption that the biological effects of hard metal particles and tungsten alloy particles would be the same.

There are no studies that address the potential health effects of internalized tungsten or HMTAs in terms of genotoxicity, mutagenicity or carcinogenicity. The long-term health risks associated with internal chronic exposure to HMTA particles are not defined but are crucial to developing carcinogenesis risk standards for personnel who could be injured by HMTA shrapnel. Therefore, in view of carcinogenesis risk estimates and medical management questions relevant to possible future incidents of tungsten internalization, an examination of molecular and cellular effects, including the potential transforming ability of tungsten and tungsten alloys, are necessary to understanding the potential carcinogenic effects of this material. The use of cell culture models to investigate potential or known carcinogens can provide important insights into the cellular and molecular mechanisms of carcinogenesis.

The *in vitro* transformation assay has not previously been used to study the transforming ability of HMTAs. This assay has been widely used in conjunction with metal salts to assess

the potential carcinogenicity of metal compounds (e.g. DU, nickel, chromium and lead) (11–15). We have therefore chosen to use this assay to initiate an assessment of the potential carcinogenicity of HMTAs. The HOS TE85 cell line, an immortalized, non-tumorigenic, osteoblast-like cell line, has been successfully used to demonstrate the transformation of non-tumorigenic human cells to the tumorigenic phenotype by metals (1,13,14) and chemical carcinogens (161,17). Several metal powders were chosen for this study. A fine tungsten powder, pure crystalline nickel, iron and cobalt were used since they are the components of one of several possible tungsten alloys used in military applications. Crystalline NiS has previously been shown to transform cells *in vitro* (13) and was tested as a positive control. Tantalum oxide (Ta_2O_5) was also used for comparison since tantalum, which is widely used in prosthetic devices, is considered an inert metal with few reported toxic effects (5).

To understand the potential health effects of internalized HMTAs used in military applications, we compared the effects of various metals that compose these HMTAs on human cell survival, transformation and induction of DNA damage. Our data demonstrate, for the first time, that a mixture of the metals used in tungsten alloys can transform human cells to the tumorigenic phenotype, similar to results observed with some DU (1) and Ni compounds (1,12–16). HMTA transformants form anchorage-independent colonies, show aberrant growth rates and produce tumors in athymic mice.

Materials and methods

Cell lines and culture

Human osteosarcoma (HOS) cells (TE85, clone F-5) were obtained from the American Type Culture Collection (Rockville, MD). Cell cultures were propagated in Dulbecco's modified Eagle's medium supplemented with 2 mM glutamine, 10% heat-inactivated fetal calf serum (Gibco Laboratories, Grand Island, NY), 100 U/ml penicillin and 100 μg/ml streptomycin (Sigma, St Louis, MO). Cells were tested for *Mycoplasma* with a MycoTect Kit (Sigma) and only cells negative for *Mycoplasma* were used.

Metal powders

The aim of the study was to examine the transforming capability of two HMTAs (tungsten/nickel/cobalt or tungsten/nickel/iron) currently used in military munitions. The weight percentage compositions of these alloys when used for military applications is approximately 91–93% tungsten, 5–3% nickel and either 2–4% iron or 2–4% cobalt (10). Since the HMTAs used by the military are not commercially available, we used a mixture of these metals, in the same percentages used by the military, to model the particles of the alloys. In this study we therefore tested the effects of a pure mixture of these materials. The powders were obtained from Alfa Aesar (Ward Hill, MA). The following powders were used: (i) extrafine cobalt metal (Alfa Aesar 10455, 99.5% purity), median particles size (d_{50}) 1–4 μm, called hereafter Co; (ii) extrafine nickel metal (Alfa Aesar 10256, 99% purity), d_{50} 3–5 μm, called hereafter Ni; (iii) extrafine iron metal (Alfa Aesar 40337, 98% purity), d_{50} 1–3 μm, called hereafter Fe; (iv) extrafine tungsten metal (Alfa Aesar 10400, 99.9% purity), d_{50} 1–3 μm, called hereafter W; (v) a pure mixture of W (92%), Ni (5%) and Co (3%) particles made in the laboratory without extensive milling, called hereafter rWNiCo; (vi) a pure mixture of W (92%), Ni (5%) and Fe (3%) particles made in the laboratory without extensive milling, called hereafter rWNiFe.

Prior to each experiment the insoluble metal particles were washed once in sterile H_2O and again in acetone. They were then suspended in acetone, agitated with a magnetic stirring bar and dispensed into cell cultures. The suspensions were carefully mixed and dispersed before being added to the cells. Dose–response experiments were conducted by altering the amounts of each metal powder, based upon its percentage of 100% of the total amount of powders. For example, 100 μg rWNiCo powder/ml consists of 92 μg W, 5 μg Ni and 3 μg Co, while 50 μg rWNiCo powder/ml consists of 46 μg W, 2.5 μg Ni and 1.5 μg Co. In this manner the total amount (weight) of metal powder mixture was varied while the ratios of the component metals were held constant.

Cellular survival assay

Cytotoxicity was assayed by measuring a reduction in plating efficiency. Exponentially growing cells were seeded at 10^4 cells/100 mm dish with three dishes per treatment group. Cultures were then treated 24 h later with 100 μl volumes of metal particles for 24 h. Cells were then rinsed with Dulbecco's phosphate-buffered saline. Cultures were detached with trypsin/EDTA and counted with a Coulter counter (Hialeah, FL). Appropriate numbers of cells (100 or 500) were then plated onto 60 mm diameter Petri dishes and cultures were returned to the incubator for 10 days to allow for colony formation. Cultures were then fixed with methanol and stained with 1% crystal violet. Plates with >15 colonies and colonies with >50 cells were counted as survivors.

Transformation and cell growth studies

For transformation assays 10^4 cells/100 mm dish were seeded and exposed to metal particles 24 h later, with three flasks per experiment. Prior to each experiment the insoluble metal particles were washed once in sterile H_2O and again in acetone. They were then suspended in acetone, agitated with a magnetic stirring bar and dispensed into cell cultures. Immediately after the 24 h metal particle exposure cells were rinsed (three times with sterile serum-free medium), trypsinized, counted and seeded in 100 mm tissue culture dishes at a density calculated to yield ~95–200 surviving cells per dish. The cultures were incubated for 5 weeks with weekly changes of nutrient medium. At the end of the incubation period cells were fixed, stained and examined for the appearance of transformed foci (18). Transformed foci were assayed using the criteria developed by Reznikoff *et al*. (18) and the modified scoring protocols were derived from Landolph (19) and the International Agency on Cancer Research/National Cancer Institute/Environmental Protection Agency (IARC/NCI/EPA) Working Group (20). The Working Group report indicated that: (i) because of the continuum of focus morphology, some foci can be intermediate (I/II or II/III) in character; (ii) these foci should be scored conservatively and assigned to the category of lower aggressive behavior. With HOS cells it was easy to distinguish between a type I and a type II focus, but somewhat difficult to differentiate between type II and type III foci. Therefore, in our experiments only type II and type II/type III foci were scored as transformants. In Table I the number of dishes with foci equals the number of foci of type II + type III. To determine the transformation frequency the Poisson formula is used, employing the first term of the Poisson distribution: $P_o = \exp(-mN)$, $m = -\ln P_o$. Details of the transformation frequency calculations and the standard error have been described elsewhere (1,21–1,22) but are detailed below. Transformed foci are not contact inhibited and may be dislodged during refeeding, forming satellite colonies. To avoid this source of errors, the average number of transformed foci per dish (λ) was computed from the proportion of dishes free of transformed colonies, f (i.e. $\lambda = -\ln f$). To determine the transformation frequency, the following formula was used:

$$\text{transformation frequency} = \lambda/\text{no. surviving cells per dish.}$$

This calculation has been widely used in radiation-induced neoplastic transformation studies to quantitatively compare transformation frequencies. The transformation data are presented from three independent experiments unless otherwise noted.

Cell survival fraction was determined using the conventional clonogenic assay (1,16). Cytotoxicity and survival assays were conducted in parallel with each transformation assay as described (1,16). Several transformed foci were picked with cloning cylinders and expanded by mass culture to establish transformed clonal lines. The transformation dose–response curve was determined as indicated above except that increasing concentrations of pure metal powders were used. The optimum dose level for transformation was selected following a preliminary toxicity test based upon colony-forming efficiency. The high dose selected resulted in >60% toxicity and the low dose selected resulted in minimal toxicity.

To determine saturation densities, cells were plated at 1×10^5 cells per 100 mm diameter plate in complete growth medium and monitored for growth as previously described (1,16). For the soft agar clonability assay cells were plated at a density of 2×10^3 cells per well in a 6-well plate sandwiched by 1 ml bottom agar (0.6%) and 1 ml top agar (0.3%). Cells were fed weekly by adding a new layer of top agar. Colonies >0.5 mm diameter were scored using a microscope after 2 weeks. The plating efficiency value for each clone represents the mean number of colonies scored from three wells. For both saturation density determination and plating efficiency in soft agar data are representative of three independent experiments. To determine DNA synthesis, incorporation of tritiated thymidine into DNA was measured as previously described (1).

Invasion through Matrigel

The ability of transformed cells to degrade and cross tissue barriers was assessed in an *in vitro* invasion assay that utilizes Matrigel, a reconstituted

Table I. Neoplastic transformation of immortalized human osteoblast cells by reconstituted tungsten heavy alloy: dose dependence

Metal	Metal content (μg/ml)	Surviving fraction	No. of dishes per experiment	No. dishes with type II and type II/type III foci	Transformation frequency per survivor[a] ($\times 10^{-4}$)
None	0	1.0 ± 0.04	155	13	4.2 ± 1.0
Co	1.5	0.96 ± 0.05	155	14	4.8. ± 1.1
Fe	1.5	0.96 ± 0.05	154	15	5.1 ± 1.2
Ni	2.5	0.93 ± 0.05	155	19	9.5 ± 1.5
W	46	0.93 ± 0.06	155	18	6.9 ± 1.8
r-WNiCo	50	0.93 ± 0.09	154	62	37.6 ± 5.1
r-WNiCo	100	0.74 ± 0.09	155	77	65.8 ± 7.1
r-WNiCo	200	0.36 ± 0.05	150	91	107.9 ± 9.1
r-WNiFe	50	0.91 ± 0.08	151	66	40.1 ± 5.5
r-WNiFe	100	0.72 ± 0.08	150	79	71.1 ± 6.5
r-WNiFe	200	0.31 ± 0.08	150	96	110.1 ± 9.5
NiS	50	0.86 ± 0.09	150	56	32.1 ± 5.1

Cytotoxicity and survival assays were conducted in parallel with each transformation assay as described (8). The transformation data are averages of three independent experiments involving ~2000 samples. The number of survivors/dish was kept to between 100 and 125 per 100 cm^2 Petri dish to avoid effects due to cell density. Transformed foci were assayed according to the criteria of Reznikoff *et al.* (18), Landolph (19) and the IARC/NCI/EPA Working Group (20) with type II and type III foci being scored as transformants. The average number of transformed foci per dish was computed from the proportion of dishes free of transformed colonies, *f*, by $\lambda = -\ln f$. Transformation frequency = λ/no. surviving cells per dish. Details of the frequency calculations and the standard errors are described elsewhere (21,22).

basement membrane (Collaborative Research, Waltham, MA). For qualitative evaluation of cell behavior 5×10^4 cells were plated onto 16 mm dishes (Costar, Cambridge, MA) which had been previously coated with 250 μl of Matrigel (10 mg/ml). The net-like formation characteristic of invasive cells occurred within 12 h; invasion into the Matrigel was evident after 4 days.

Alkaline phosphatase (ALP) activity

The percentage of cells exhibiting ALP activity on their cell surface was evaluated on cytospins obtained 4 days after cell seeding using a cytochemical method (Kit 86R; Sigma) (23). The percentage of cells was calculated on at least 350 cells. Cellular ALP activity was also analyzed 4 days after seeding. Approximately 10^6 cells were resuspended in homogenization buffer (1 mmol/l $MgCl_2$, 1 mmol/l $CaCl_2$, 20 mol/l $ZnCl_2$, 0.1 mol/l NaCl, 0.1% Triton X-100, 0.05 mol/l Tris–HCl, pH 7.4) and disrupted by gentle vortexing. The homogenate was used for the ALP assay, which was performed with *p*-nitrophenol phosphate as substrate as per the Kit 86R instructions. L/B/K ALP activity was normalized for the content of protein in the sample. Protein was measured using the Bradford method (1,2). One unit of L/B/K ALP activity is defined as the amount of enzyme capable of transforming 1 μmol substrate in 1 min at 25°C.

Tumorigenicity assay

Experiments were performed with 4–5 week old female athymic mice (Division of Cancer Treatment, NCI Animal Program, Frederick Cancer Research Facility, Frederick, MD). For this assay 5×10^6 cells in a 0.2 ml sterile suspension were injected s.c. in the right scapula. Animals were then observed for tumor growth at the sites of injection for 180 days. Tumor area was measured using a caliper measurement of two perpendicular diameters. When tumors were >100 mm^2 the animal was killed.

Northern blot analysis and DNA probes

Cytoplasmic RNA was extracted from exponentially growing cells and separated by electrophoresis in 1% agarose–formaldehyde gels. RNA preparation and blotting onto nytran filters, hybridization with radiolabeled DNA probes and autoradiography were previously described (1,16). The *ras* probe, a *Sac*I 2.9 kb fragment of the human *ras* gene, and a 1.8 kb fragment of the human β-actin gene were obtained from Oncor (Gaithersburg, MD). ^{32}P-labeled DNA probes were prepared using a random primed DNA labeling kit (Boehringer Mannheim, Indianapolis, IN).

Micronuclei (MN) analysis

The induction of MN in control- and metal powder(s)-exposed cells was assessed using the conventional fluorescence plus Giemsa harlequin staining protocol (24). Following a 1 h exposure, the medium containing the metal powder was removed and cells were rinsed (three times with sterile serum-free medium) and incubated again at 37°C in complete medium. Mitomycin C was used as a positive control (24 h exposure). Cytochalasin B (6 μg/ml) was added after 24 h to block cytokinesis. At 48 h post-treatment cells were dropped onto slides using a cytospin (Shandon, St Louis, MO) for 5 min at 600 r.p.m. Slides were fixed with 5% Giemsa.

Alkaline elution test

The DNA breakage potencies of the metal powders were examined using the rapid alkaline elution test based on the method of Kohn *et al*. (25) and using the Millipore Multiscreen Assay System as described by Anard and co-workers (26). A 96-well filtration plate with a hydrophilic polyvinylidene fluoride microporous membrane (pore size 0.65 μm) sealed to its bottom was used along with a vacuum manifold to remove solutions from the filters. Cells were labeled for 18 h with 1 μCi/ml [^{3}H]TTP (ICN, Costa Mesa, CA) prior to analysis of DNA damage by alkaline elution. Approximately 7×10^4 labeled cells were dispersed into each well of the filtration plate and exposed to the different powders suspended in complete medium. After 1 h exposure 1 mM sodium formate was added and the cells were lysed in a solution containing 0.04 M Na_4EDTA, 2 M NaCl, 0.2% *N*-lauroylsarcosine, 0.5 mg/ml proteinase K and 1 M sodium formate, pH 9.0. The DNA remaining on the filters was washed with a solution containing 0.02 mM Na_4EDTA. Elution buffer (0.1 M tetrapropylammonium hydroxide, 0.02 M EDTA, pH 12.1) was added in a volume of 300 μl and the DNA was eluted by vacuum (~16 kPa) in a single fraction. The DNA breakage potency of the different powders was assessed by quantifying the radioactivity recovered with the eluted fraction.

Histopathology of tumors

For routine staining, tumor tissues were fixed in buffered 10% formalin, embedded in paraffin, sectioned and stained by routine hematoxylin and eosin methods (1,16).

Statistics

Statistics for the MN and alkaline elution assays were performed with the χ^2 test and the Tukey–Kramer multiple comparisons test, respectively.

Results

Characterization of the model system: heavy metal powder cytotoxicity

An assessment of metal powder exposure on cell growth and survival was done to initially characterize our HOS model system and to determine suitable amounts of metal powders to be used in the transformation studies. Cytotoxicity data were computed relative to control (untreated) cultures. Figure 1 compares the effect of increasing concentrations (0.75–200 μg powder/ml) of the various powders (W, Ni, Co, Fe or the reconstituted mixtures rWNiCo and rWNiFe) on HOS cell survival. Colony formation data demonstrated that cellular exposure to either the pure powders (W, Ni, Co or Fe) or the reconstituted powders (rWNiCo or rWNiFe) induced a dose-dependent decrease in cell survival (Figure 1). At concentrations up to 2.5 μg powder/ml Co, Ni and Fe were non-toxic,

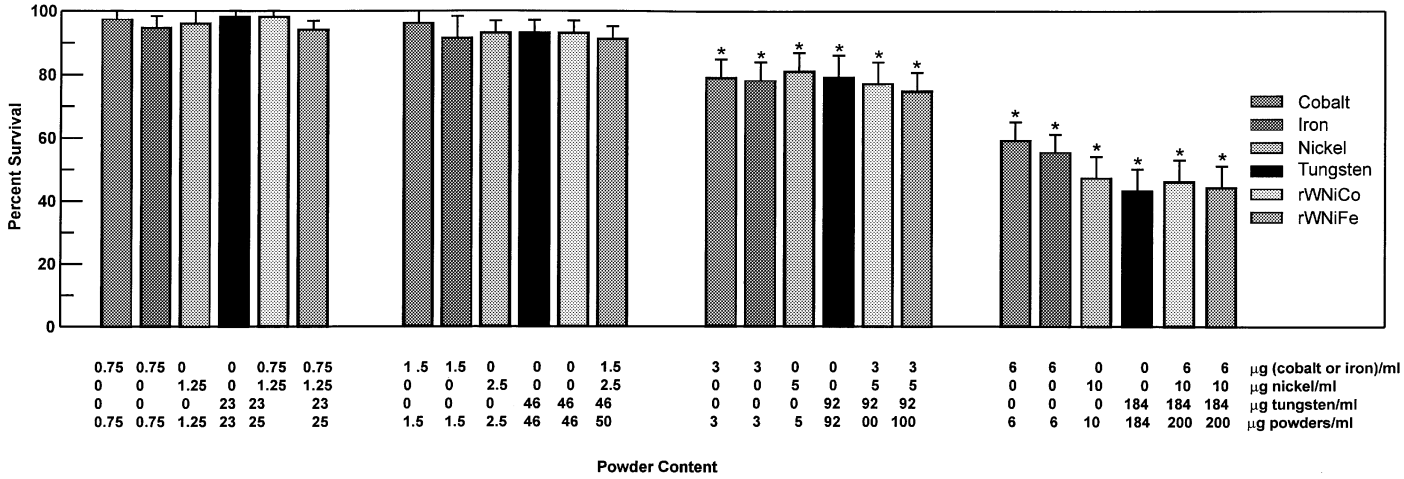

Fig. 1. Effect of various metals (tungsten, nickel, cobalt, iron, tungsten + nickel + cobalt mixture and tungsten + nickel + iron mixture) on HOS cell survival following a 24 h exposure. Data are means ± SD from three experiments.

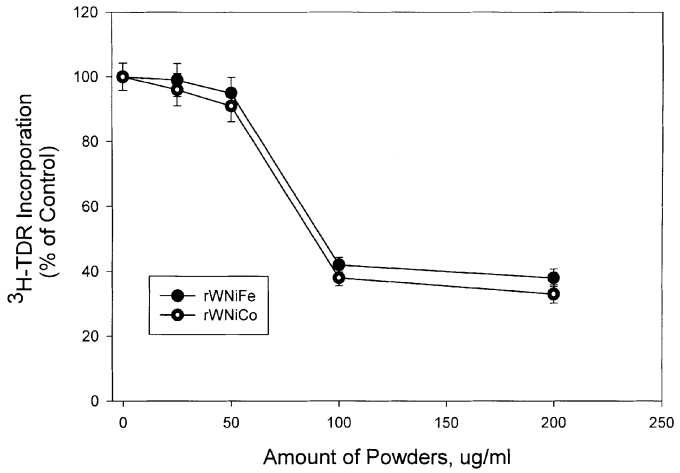

Fig. 2. Effect of the tungsten alloy mixtures (rWNiCo and rWNiFe) on DNA synthesis. HOS cells were incubated for 24 h with rWNiCo or rWNiFe (0–200 µg powder/ml). During the last 4 h of incubation [^{3}H]thymidine was added to the medium. Each point corresponds to the mean of three estimations of acid-precipitable radioactivity at each amount of metal mixture powder, expressed as a percentage of the untreated control. Error bars denote SD. $P < 0.001$ relative to untreated control in Student's *t*-test.

while W and the reconstituted tungsten powders were non-toxic at concentrations up to 46–50 µg powder/ml. The LD_{50}, determined from a series of plots (survival percentage versus powder amount/ml; data not shown) was ~7–10 µg powder/ml for Co, Ni and Fe and 185–200 µg powder/ml for W, rWNiCo and rWNiFe.

The effect of rWNiCo and rWNiFe on cell proliferation, measured as tritiated thymidine incorporation into DNA, is shown in Figure 2. Both rWNiCo and rWNiFe inhibited thymidine incorporation in HOS cells in the range 50–200 µg powder/ml in a dose-dependent manner. Experiments were conducted under optimal growth conditions, i.e. in the presence of 10% fetal calf serum. Growth rate analysis by cell enumeration (data not shown) demonstrated similar results.

To preclude excessive cell killing or proliferation effects due to heavy metal toxicity, the non-toxic, non-cytostatic concentration of both rWNiCo and rWNiFe chosen for the transformation experiment was 50 µg powder/ml (24 h exposure, surviving fraction 95.5 ± 5%). To establish transformation dose–response curves for these powders, two additional powder concentrations that manifest ~75 (100 µg powder/ml) and 35% (200 µg powder/ml) cell survival were also chosen.

Transformation of HOS cells by rWNiCo and rWNiFe: comparison with pure W, Ni, Co and Fe

To assess morphological cell transformation, the standard focus formation assay previously described by others for both C3H/10T1/2 and HOS cells was used (1,11–19); we also previously used this assay to examine the effects of DU on HOS cells (1). Based on our toxicity and growth data we selected a non-toxic and non-cytostatic exposure of the two metal mixtures to examine their transforming potentials. The morphology of untreated and rWNiCo-treated HOS cells is shown in Figure 3. HOS cells exhibit a flat epithelial-like morphology and appear to grow in a monolayer (Figure 3A). In contrast, exposure to rWNiCo caused a morphological change in HOS cells (Figure 3B). Following treatment with rWNiCo and weekly changes of nutrient medium for 5 weeks, diffused type II foci appeared (Figure 3B). The morphology of the foci is distinctly different from the surrounding cells (Figure 3b). The foci exhibit a slight multi-layered pattern, which is somewhat different from the 'piled up' appearance seen in transformed C3H10T1/2 cells (1,16–18). Similar morphological changes were observed for cells exposed to rWNiFe (data not shown). The transforming potential of each pure metal was also tested. Table I shows measured values for the transformation frequencies (normalized per surviving cell) for HOS cells treated with W (46 µg/ml), Ni (2.5 µg/ml), Co (1.5 µg/ml), Fe (1.5 µg/ml), rWNiCo (50–200 µg powder/ml) and rWNiFe (50–200 µg powder/ml). The data demonstrate that treatment with rWNiCo and rWNiFe resulted in a transformation frequency of $37.6 \pm 3.90 \times 10^{-4}$ and $40.1 \pm 3.85 \times 10^{-4}$, respectively. These increased transformation frequencies represent 8.90 ± 0.93- and 9.50 ± 0.91-fold increases in transformation frequency, respectively, compared with the frequency in untreated HOS cells. In comparison with rWNICo and rWNiFe, cellular exposure to the pure powders W, Co and Fe (1.5–184 µg/ml) did not significantly increase the transformation frequency above untreated control levels (Table I). Data are not shown for Co and Fe (3 and 6 µg/ml) and W (92 and 184 µg/ml). Incubation with pure nickel (2.5, 5, 10 µg/ml), however, did result in a small but statistically significant increase in transformation frequency (control, $4.21 \pm 0.41 \times 10^{-4}$;

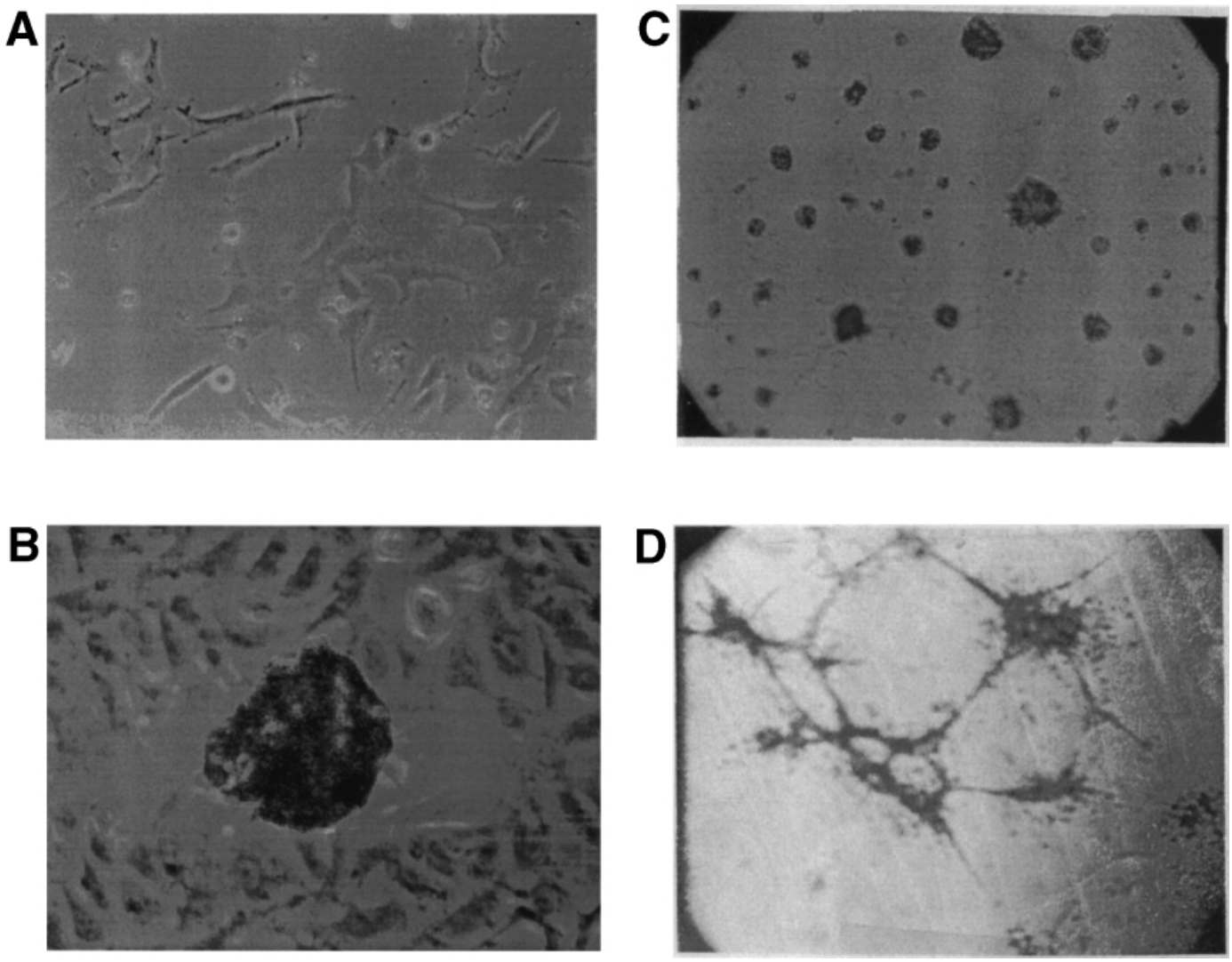

Fig. 3. Morphology of HOS cells and focus formation following rWNiCo exposure and growth of cells in matrigel. Phase contrast micrograph, magnification ×40. (**A**) Morphology of control HOS cells. (**B**) Focus formation in HOS cells. The edge of a focus of transformed cells is seen against a background of parental HOS cells with normal morphology. (**C**) Growth of control HOS cells in matrigel. (**D**) Growth of rWNiCo transformants in matrigel.

2.5 μg/ml, 7.55 ± 0.75×10^{-4}; 5 μg/ml, 9.11 ± 0.95 ×10^{-4}; 10 μg/ml, 10.55 ± 1.85×10^{-4}). Data in Table I are only shown for the lowest amount of pure nickel. In comparison, cellular exposure to a higher dose of the known transforming agent crystalline NiS (50 μg/ml) increased the transformation frequency to 32.5 ± 3.10×10^{-4}. Not only has Ni exposure been epidemiologically linked to cancer but the ability of Ni to transform cells *in vitro* was previously demonstrated by this laboratory and others and is shown here for comparison (1,12–14). In contrast, the biologically inert Ta_2O_5 did not induce an increase in HOS transformation frequency above untreated levels (Table I). These data also demonstrated a metal dose-dependent increase in transformation frequency. Several rWNiCo- and rWNiFe-transformed foci were picked with cloning cylinders and expanded by mass culture to establish transformed clonal lines. A spontaneous focus arising from untreated HOS cells was also selected and expanded. These transformed clones were selected for growth analysis (invasiveness in Matrigel; saturation density; growth in agar), ALP activity and tumorigenicity.

The cellular potential for invasion through reconstituted basement membrane Matrigel was assessed using untreated HOS cells and metal transformants. A comparison of these cells is shown in Figure 3 for untransformed parental HOS cells (Figure 3C) and a single rWNiCo transformant (Figure 3D). The rWNiCo transformant grew in Matrigel developing characteristic net-like structures, eventually degrading the extracellular matrix components. In marked contrast, untransformed parental HOS cells formed small non-invasive colonies on top of the Matrigel. The spontaneously transformed HOS cells were not used in this assay.

Biological characterization of the transformed phenotype

Alteration in growth control is critical to neoplastic transformation and therefore the rWNiCo- and rWNiFe-transformed clones were further characterized by quantitative differences in growth properties associated with the neoplastic phenotype, e.g. saturation density and soft agar colony-forming efficiency. Additionally, ALP activity and tumorigenicity were assessed in untreated and transformed HOS cells.

The saturation densities of rWNiCo- and rWNIFe-transformed cells were approximately three times higher than that of the parental HOS cells (Table II). Saturation density data obtained for cells treated with W, Ni, Co and Fe powder were

Table II. Biological and biochemical properties of HOS cells transformed by rWNiCo and rWNiFe: saturation density, plating efficiency in soft agar and alkaline phosphatase activity

Metal/clone transformant	Saturation density[a] (no. cells × 10^5)	Growth in soft agar[b]		Alkaline phosphatase activity[c]	
		Plating efficiency in soft agar (%)	Colony size (mm)	Expression of membrane-bound ALP (% positive cells/total)	Membrane-bound ALP activity (mU/mg protein)
None/control	2.6 ± 0.15	3 ± 1.0	> 0.5	100	97.5 ± 7.9
Co	2.9 ± 0.18	1 ± 0.30	> 0.5	100	93.2 ± 8.6
Fe	3.0 ± 0.22	3 ± 1.0	> 0.5	100	102.2 ± 9.7
Ni	3.5 ± 0.25	8 ± 0.80	> 0.5	97	83.4 ± 7.1
W	3.2 ± 0.20	8 ± 0.80	> 0.5	100	88.0 ± 7.4
rWNiCo	7.2 ± 0.66	34 ± 3.4	> 0.5	11	3.22 ± 2.0
rWNiFe	7.3 ± 0.62	47 ± 4.9	> 0.5	7	2.4 ± 1.9

[a]To determine saturation densities cells were plated at 1×10^5 per 100 mm diameter plate in complete growth medium and monitored for growth as previously described (8).
[b]For the soft agar clonability assay cells were plated at a density of 2×10^3 per well in a 6-well plate sandwiched by 1 ml bottom agar (0.6%) and 1 ml top agar (0.3%). Cells were fed weekly by adding a new layer of top agar. Colonies of >0.5 mm diameter were scored using a microscope after 4 weeks. The plating efficiency value for each clone represents the mean number of colonies scored from three wells. For both saturation density determination and plating efficiency in soft agar data are representative of three independent experiments.
[c]*In vitro* ALP activity was measured 4 days after seeding.

similar to that for parental HOS cells. An assessment of anchorage-independent growth ability was also done. A comparison of the transformants ability to grow in soft agar revealed that the rWNiCo and rWNiFe transformants generated colonies within 1 week with colony-forming efficiencies of 34 and 47%, respectively. Parental HOS cells and cells treated with the pure metals did not form a significant number of colonies in soft agar (Table II). We have previously shown that DU, *N*-methyl-*N′*-nitro-*N*-nitrosoguanidine and EJ-*ras* transformants formed soft agar colonies whose size and frequency were comparable with those observed with the rWNiCo and rWNiFe transformants (1,15).

Since ALP activity was recently shown to correlate with the malignant phenotype in transformed HOS cells (23), it was also evaluated in control, metal-treated and transformed HOS cells. Parental HOS cells and HOS cells treated with each of the pure metals showed positive staining for ALP in all of the cells and high levels of cellular ALP activity (Table II). In contrast, rWNiCo and rWNiFe transformants exhibited a low percentage of cells positive for ALP activity and low cellular ALP activity.

Inoculation of athymic nude mice with rWNiCo and rWNiFe transformants resulted in the development of animal tumors at the site of injection within 4 weeks (Table III). In contrast, parental HOS cells and cells treated with W, Ni, Co or Fe (46, 2.5, 1.5 and 1.5 μg powder/ml, respectively) injected into nude mice did not result in tumor formation during a period of 6 months after cell inoculation. Tumor tissue was excised and used for histochemical and immunohistochemical analyses. Some tumor tissue was also used to establish cell lines for further study.

Histological examination of the tumors formed by rWNiCo revealed an infiltrative neoplasm consisting of cuboidal cells forming acini, papillary fronds and tubules (Figure 4). No neoplastic spindled cells were present. This diagnosis suggests adenocarcinoma, a malignant epithelial neoplasm. Immunohistochemistry for cytokeratin, an epithelial marker, and for vimentin, a mesenchymal marker, were 'positive' and 'negative', respectively (Figure 4). Microscopic examination of sections of these tumors revealed tumor tissue similar to that

Table III. Tumorigenicity of HOS cells transformed by tungsten/nickel/cobalt

Metal	No. cells injected per mouse ($\times10^6$)	Latency period[a] (days)	Tumor incidence[b]
None/control	5		0/128
Co	5		0/12
Fe	5		0/12
Ni	5		0/12
W	5		0/12
rWNiCo	5	26	6/12
rWNiFe	5	24	7/12

[a]Time between injection of cells and detection of palpable tumors. Animals were examined three times a week for tumors. After tumor palpation animals were examined five times a week until the animals were killed (tumor volume ~90 mm^2).
[b]Number of mice developing tumors/total number of mice inoculated. Examined tumors were identified as adenocarcinomas. See Discussion for further details.

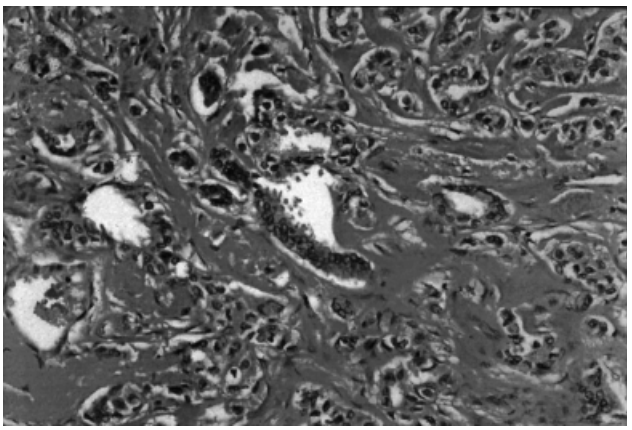

Fig. 4. Histopathology of tumors growing in nude mice following injection of rWNiCo-transformed cells. H&E, original magnification ×212.

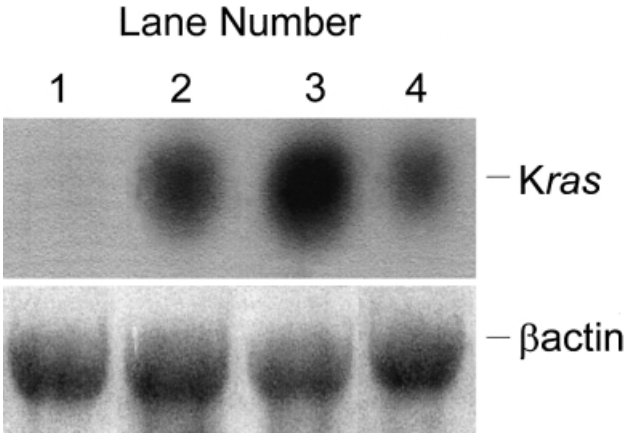

Fig. 5. Analysis of *ras* oncogene expression in parental HOS, rWNiCo-, rWNiFe- and EJ-*ras*-transformed clones. Data are representative of three separate experiments. Northern blot analysis of cytoplasmic RNA (20 μg): lane 1, HOS; lane 2, rWNiCo-transformed cells; lane 3, rWNiFe-transformed cells; lane 4, EJ-*ras*-transformed cells. (Upper) Hybridization with a ^{32}P-labeled K-*ras* probe (*ras* transcripts were undetectable in HOS cells). A *Sac*I 2.9 kb fragment of the human *ras* gene and a 1.8 kb fragment of the human β-actin gene were used. (Lower) Hybridization with ^{32}P-labeled actin was used to indicate that the relative amounts of RNA loaded into each lane were the same.

observed with tumors induced by neoplastic transformation of HOS cells by DU (1) and NiS (14). Tumors were re-established in tissue culture and confirmed as human; their resemblance to the cells of origin was determined by karyological analysis (not shown) (1,16). These re-established cells were also assayed for the formation of mineralized matrix. Transformed cells grown in matrix development medium showed weak diffused staining for alkaline phosphatase and $Ca_3(PO_4)_2$. A similar pattern of growth and staining was observed for DU-transformed cells (1; Table II). This diagnosis is similar to that previously observed with metal- and chemical-transformed HOS cells (1,3).

ras analysis in HMTA transformants

Neoplastic cell transformation is hypothesized to result from a multi-step process involving activation of oncogenes and inactivation of tumor suppressor genes (27). Both metal- and radiation-induced neoplastic transformation has been shown to be associated with genetic alterations in specific oncogenes and tumor suppressor proteins, e.g. *ras* (1,12,16). Therefore, possible molecular changes in *ras* associated with HMTA-induced transformation were studied using rWNiCo- and rWNiFe-transformed cell lines. Northern blot analysis, shown in Figure 5, revealed high levels of K-*ras* mRNA in each of the HMTA clones tested. In contrast, K-*ras* mRNA levels were undetectable in parental HOS cells. The level of EJ-*ras* mRNA in EJ-*ras*-transformed HOS cells is also shown for comparison. The amount of actin mRNA was similar in all clones tested (bottom).

Micronucleus induction in HOS cells exposed to rWNiCo, rWNiFe, W, Ni, Co and Fe

The MN test was used to assess the ability of the metal powders to induce chromosomal aberrations (chromosome/genome mutations) and hence their genotoxic potential. MN induction in HOS cells after treatment with the pure or reconstituted powders was analyzed at each concentration (Table IV). Mitomycin C, a known inducer of MN, is shown for comparison. The frequencies of micronucleated cytokinesis-blocked (MN-CB) HOS cells treated for 1 h with metal particles and harvested after 48 h are presented in Table IV for each powder and reconstituted mixture. There was a statistically significant increase in MN-CB observed with each metal tested in comparison with untreated cells. For the reconstituted mixtures, rWNiCo and rWNiFe, a dose-dependent, statistically significant increase in MN-CB was observed.

Table IV. Micronucleus induction in HOS cells exposed to Co, Fe, Ni, W or mixture rWNiCo or rWNiFe: comparison with mitomycin C

Metal	Concentration (μg/ml)	MN-CB cells (%)	No. MN-CB cells analyzed	Percent MN-CB (mean ± SE)
Control	0	34.5	100	7.0 ± 0.07
Co	0.75	21.1	100	22.5 ± 2.0[a]
	1	23.2	100	19.1 ± 2.0[a]
	3	22.9	100	32.5 ± 3.1[a]
	6	23.4	100	42.9 ± 5.0[a]
Fe	0.75	23.1	100	25.5 ± 2.0[a]
	1	27.2	100	22.1 ± 2.0[a]
	3	22.9	100	33.5 ± 3.1[a]
	6	29.4	100	40.9 ± 5.0[a]
Ni	1.25	33.1	100	22.8 ± 2.2[a]
	2	33.8	100	23.3 ± 1.9[a]
	5	35.5	100	41.0 ± 4.3[a]
	10	32.1	100	46.3 ± 2.2[a]
W	23	29.6	100	17.9 ± 1.9[a]
	46	27.5	100	24.5 ± 2.6[a]
	92	24.6	100	21.3 ± 2.0[a]
	184	29.1	100	22.7 ± 2.1[a]
rWNiCo	25 (1.25/0.75/23)[b]	17.1	100	25.4 ± 1.9[a]
	50 (2/1/46)	20.3	100	55.5 ± 5.6[a]
	100 (5/3/92)	24.8	100	82.8 ± 7.8[a]
	200 (10/6/184)	22.6	100	67.1 ± 6.1[a]
rWNiFe	25 (1.25/0.75/23)	21.1	100	29.4 ± 2.0[a]
	50 (2/1/46)	20.7	100	58.5 ± 5.8[a]
	100 (5/3/92)	25.5	100	89.8 ± 7.8[a]
	200 (10/6/184)	24.7	100	77.1 ± 7.1[a]
Mitomycin C	0.20	33.3	100	73.9 ± 6.4[a]

[a]Statistical differences were determined with the χ^2 test. $P < 0.01$ (significant difference between control and treated cultures).

Induction of DNA breaks in HOS cells exposed to rWNiCo, rWNiFe, W, Ni, Co and Fe

The induction of DNA breaks in HOS cells after exposure to the pure metals or the reconstituted mixtures was measured at each concentration using the alkaline elution assay (Figure 6). Pure Co, Ni and Fe particles induced a small but statistically significant dose-dependent increase in the production of DNA breaks. In contrast, W alone did not induce any significant DNA breakage. The DNA breakage potency of the individual metals was, however, significantly less than that of either rWNiCo or rWNiFe. At the highest dose tested cellular exposure to either rWNiCo or rWNiFe yielded an increase in DNA breaks of 850–900% above untreated levels. The induction of DNA breakage by the metal mixtures appeared to be synergistic since the sum of the breakage increase for all the pure metals was less than that for the reconstituted mixture.

Discussion

This study was undertaken to assess the transforming and genotoxic potential of two heavy metal–tungsten alloy metals used in military munitions. Since these tungsten alloys are not commercially available, we used a mixture of the pure metals that compose each heavy metal–tungsten alloy. These metal

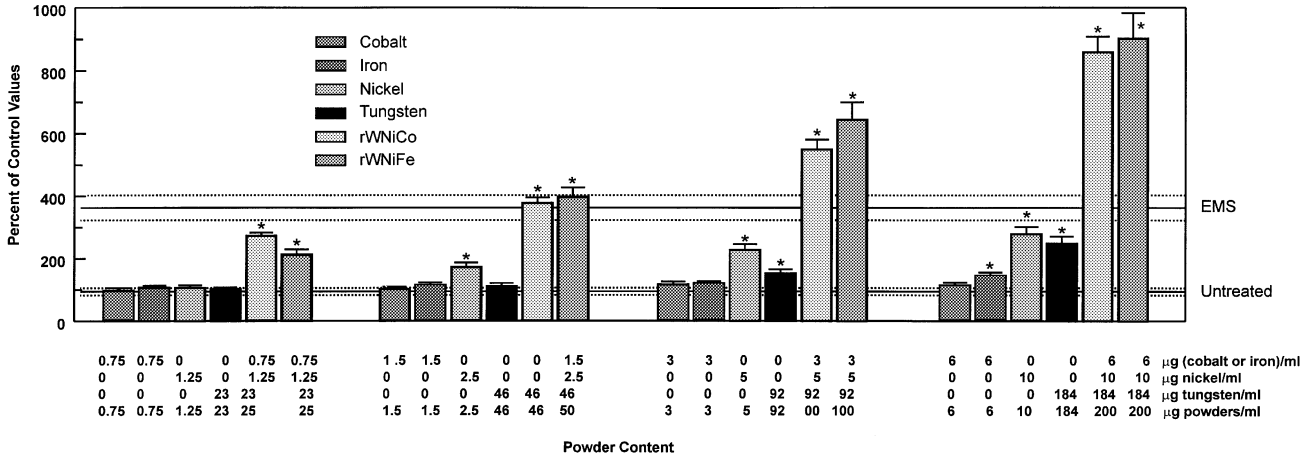

Fig. 6. DNA single-strand break analysis using alkaline elution of HOS cells exposed to various metals (tungsten, nickel, cobalt, iron, tungsten + nickel + cobalt mixture and tungsten + nickel + iron mixture) for 1 h. Results are the means ± SD from three determinations. The control (unexposed HOS cells) and the positive control (100 mM ethyl methyl sulfonate) are represented by three horizontal lines (mean ± SD). Error bars denote SD. $P < 0.001$ relative to untreated control in Student's *t*-test.

mixtures, which mimic the ones used in military applications, are composed of tungsten, nickel and cobalt or tungsten, nickel and iron.

Our studies demonstrate for the first time that the malignant transformation of immortalized human cells can be achieved by exposure to a mixture of W, Ni and Co or a mixture of W, Ni and Fe. Transformants with both metal mixtures showed morphological changes, anchorage-independent growth in soft agar, induced tumors when transplanted into nude mice and exhibited alterations in *ras* oncogene expression. Cellular exposure to these mixtures also induced DNA breakage and chromosomal aberrations, i.e. MN induction, indicating that these mixtures are genotoxic. This is the first report to demonstrate not only that a tungsten alloy mixture can transform human cells, but also that, based upon equivalent concentrations and metal toxicities, the magnitude of this transformation is ~1.3-fold greater than that observed for NiS, a well-known transforming agent and carcinogen (13). Furthermore, both rWNiCo and rWNiFe caused a dose-dependent increase in the transformation frequency of HOS cells. Since there are little data regarding the potential tumorigenic and genotoxic effects of internalized tungsten and tungsten alloys, these results are important to the understanding of the mechanism of the potential late health effects, i.e. carcinogenicity, of tungsten alloys used in military applications.

These studies also confirm previous results demonstrating that HOS cells can be used to assess quantitative transformation in addition to morphological and neoplastic transformation (1,13,14,16). Morphological transformation studies have primarily involved rodent cell lines such as C3H and 10T1/2 (11,15). As with our previous DU studies (1), our current results again demonstrate that human cell models are available not only for morphological but also for quantitative transformation studies. The current studies with tungsten alloy mixtures demonstrate another step in understanding the transformation process of HOS cells.

The precise mechanism(s) by which rWNiCo and rWNiFe induce transformation in HOS cells is not fully known, although the data suggest several possibilities. Alterations in specific oncogenes (e.g. *ras*) and/or inactivation of tumor suppressor genes (e.g. *p53*) involved in the conversion of these cells to the malignant phenotype have been considered. HOS cells contain a mutation at codon 156 of the *p53* gene, resulting in a mutated form of p53 protein that is believed to be partially responsible for their immortalization (28). Since neoplastic conversion is postulated to result from a multi-step process involving cell immortalization and gene alterations (27,29–31), transformation of immortalized HOS cells by rWNiCo and rWNiFe to the malignant phenotype may involve other cellular oncogenes in this process. Our data demonstrate that the *ras* oncogene was activated in the transformation process induced by both rWNiCo and rWNiFe exposure. The *ras* oncogenes have been implicated in both chemical- and radiation-induced animal tumors (1,29–32) and in spontaneous human tumors (33). Studies also show that the c-*myc* protooncogene plays an important role in the nickel- and lead-induced transformation of mammalian cells, possibly by stabilizing protooncogene RNAs (34,35). Additionally, effects on tumor suppressor proteins have also been observed in metal-transformed clones. DU- (1) and Ni-induced (1,12) transformations of HOS cells were both shown to affect the encoded protein of the *Rb* tumor suppressor gene by altering phosphorylation of Rb protein in the transformed clones. Similarly, long-term exposure of human epithelial cells to nickel resulted in *p53* gene point mutations (35). Considering these findings, we speculate that the transformation of human cells by tungsten alloy mixtures may result from a conversion process that definitely involves activation of tumor-promoting gene(s) and that may involve alterations in tumor suppressor proteins. This hypothesis awaits further testing.

Histological and histochemical analyses of tumors formed by both the rWNiCo- and rWNiFe-transformed cells indicated a gland-like pattern with random calcium deposition rather than an osteogenic sarcoma pattern of growth. Specifically, this histological tumor examination revealed an infiltrative neoplasm consisting of cuboidal cells forming acini, papillary fronds and tubules with no neoplastic spindled cells present, which is consistent with a diagnosis of adenocarcinoma. The finding of a malignant epithelial neoplasm rather than a sarcoma, a malignant mesenchymal neoplasm, was not expected. However, transformation of a spindled cell line, like HOS, with subsequent transplantation into nude mice may result in dedifferentiation at some point, resulting in growth of an epithelial neoplasm. A previous study of NiS-induced

transformation of HOS cells reported the same unexpected histomorphology of neoplasms in recipient nude mice; that study also included supportive immunohistochemistry with positive cytokeratin and positive carcinoembryonic antigen staining, both epithelial markers (14). Furthermore, in our study untreated HOS cells formed ALP-positive foci which calcified on extended culture, while the HMTA-transformed cells lacked the ability to form multilayered cellular structures and ALP-positive foci. Changes in ALP activity have been shown to be associated with expression of the malignant phenotype in human osteosarcoma cells (23). Additionally, both rWNiCo- and rWNiFe-transformed cells deposited calcium randomly in areas showing clumped growth of cells. Taken together, these observations suggest that HMTA-transformed cells had dedifferentiated and lost some osteoblastic characteristics. The similarity of our results to previous studies of HOS transformation and tumorigenesis strongly suggests that HOS tumorigenic cells dedifferentiate *in vivo* (1,14).

As indicated previously, the tungsten alloy mixtures and the pure metals (except Ni) have not been tested for transforming potential. However, studies addressing hard metal lung disease examined the cytotoxic and cytogenetic effects of Co, WC and a WC + Co mixture (36,37). The results demonstrated that WC + Co had a greater cellular toxicity than pure Co metal particles (8,9) and that cellular uptake of Co was enhanced when it was present in the form of WC + Co. The increased toxicity did not result from the increased bioavailability of Co, however, and it appears that WC + Co behaved as a specific toxic entity (9,35–37). Similarly, our data also show that the tungsten alloy metal mixtures W/Ni/Co and W/Ni/Fe exhibit a greater toxicity than that of any of the pure metals. We have not yet determined whether there is any enhanced bioavailabilty of any of the pure metals in the mixture or whether this potentially increased bioavailability would affect the toxicity or transforming ability of the tungsten alloy mixtures. Ongoing studies on HMTA uptake and bioavailability may help to answer these questions.

The mechanism by which rWNiCo and rWNiFe induce cell transformation *in vitro* appears to involve, at least partially, direct damage to the genetic material, manifested as increased DNA breakage and chromosomal aberrations (i.e. MN). Our data clearly show that direct DNA damage and induction of chromosomal aberrations result from cellular exposure to the tungsten alloy mixtures. In contrast, only the highest doses of pure W, Ni and Co induced any significant increase in DNA breakage above background. Ni and Co were previously shown to be genotoxic at higher, toxic concentrations (38), so our data with Ni and Co at low, non-toxic doses are not too surprising. The HMTA mixtures demonstrate a synergistic increase in DNA breakage when the pure metals are mixed together to compose the tungsten alloy mixture. In contrast, MN induction by the HMTA mixtures, while significantly greater than the level of MN induction by each pure metal, did not exhibit a synergistic relationship. The MN test may be somewhat less sensitive in assessing the synergistic DNA-damaging potential of the mixture demonstrated by the DNA breakage assay. The MN assay does, however, detect chromosomal aberrations and not just repairable DNA breakage. Therefore, the combination of the DNA single-strand break and MN assays provides a better understanding of the mechanisms responsible for the genotoxic nature of the HMTA mixtures.

Other mechanisms may be involved by which rWNiCo and rWNiFe induce cell transformation *in vitro*. Studies have demonstrated that non-genotoxic, carcinogenic metals like lead may induce transformation via an indirect mechanism such as changes in DNA conformation or enzymatic disturbances (39). Other studies have also demonstrated that inhibition of DNA replication, leading to an elevation in sister chromatid exchanges, may be involved in metal-induced transformation (40,41). All of these mechanisms could potentially be involved in the HMTA transformation process, since transformation induced by metals like Ni appears to involve multiple mechanisms essential to the neoplastic process. For example, the involvement of epigenetic mechanisms of action has also been postulated for Ni. Chromatin condensation, *de novo* methylation and the resultant aberrant genetic activity may be partially responsible for the carcinogenic action of Ni (34,42). Similarly, recent unpublished data from our laboratory demonstrate that cellular exposure to rWNiCo resulted in hypermethylation of DNA (unpublished data). Although we do not have any direct evidence that neoplastic transformation by the HMTA mixtures involves epigenetic mechanisms, we cannot rule out their potential involvement in the transformation process.

Another possible mechanism in HMTA mixture transformation may involve reactive oxygen species (ROS). The formation of oxygen radicals in metal transformation is well documented, however, for some metals the contribution of these free radicals to the carcinogenic process is somewhat unclear (38). For Ni it is clear that ROS are involved. On a cellular level, Ni has been shown to increase protein oxidation and induce formation of cell oxidants (42) and the binding of Ni to peptides increases its accessibility to critical DNA sites. Animal studies have confirmed the role of Ni and Ni-mediated ROS in the mechanism of Ni carcinogenesis (43). Similarly, Fe potentiates oxygen toxicity via the Fenton reaction, producing hydroxyl radicals and inducing oxidative stress (44). Animal carcinogenesis studies provide evidence that high doses of Fe are also carcinogenic (45). In contrast, Co, which also generates substantial amounts of oxygen radicals, is not mutagenic or carcinogenic (46). When Co and WC particles are mixed together, however, hydroxyl radicals are generated that contribute to the mixture's induction of DNA damage (9,37). Epidemiological studies demonstrate that occupational exposure to hard metals may cause different types of lung diseases (6,7), including cancer (47). Based on these findings with other metals, it is interesting to speculate that another mechanism by which the HMTA mixtures induce transformation, chromosomal aberrations and DNA breakage may involve oxidative damage. This hypothesis awaits further testing.

In summary, we used a model system of *in vitro* human osteoblast cells exposed for 24 h to rWNiCo (50 μg powder/ml) and rWNiFe (50 μg powder/ml) to assess the relative transforming potential of HMTAs in an effort to better understand the potential health risks from long-term exposure to internalized HMTAs. Cellular exposure to HMTAs induces neoplastic transformation. These HMTA transformants are characterized by anchorage-independent growth, tumor formation in nude mice and expression of high levels of the K-*ras* oncogene. The mechanism by which rWNiCo and rWNiFe induce cell transformation *in vitro* appears to involve, at least partially, direct damage to the genetic material manifested as increased DNA breakage or chromosomal aberrations (i.e. MN). These HMTAs appear to have transforming ability somewhat greater than that of many other trace heavy metals which also induce neoplastic cell transformation *in vitro* as well as cause tumor formation in animals (42). While additional

animal studies are needed to address the effect of protracted exposure and tumor induction *in vivo*, the implication from our model system study is that the risk of neoplastic induction from internalized HMTA exposure may be similar to other biologically reactive and carcinogenic heavy metal compounds (e.g. Ni).

Acknowledgements

The authors are grateful for the helpful guidance and assistance of Drs David McClain and John Kalinich. We also thank Dr David Ledney for his suggestions. This research was supported in part by the Armed Forces Radiobiology Research Institute under work unit no. AFRRI-99-4. The views presented are those of the authors and do not necessarily reflect the official views of the Department of Defense or the US government.

References

1. Miller,A.C., Blakely,W.F., Livengood,D., Whittaker,T., Xu,J., Ejnik,J.W., Hamilton,M.M., Parlette,E., St. John,T., Gerstenberg,H.M. and Hsu,H. (1998) Transformation of human osteoblast cells to the tumorigenic phenotype by depleted uranium-uranyl chlroide. *Environ. Health Perspect.*, **106**, 465–471.
2. Miller,A.C., Fuciarelli,A.F., Jackson,W.E., Ejnik,E.J., Emond,C., Strocko,S., Hogan,J., Page,N. and Pellmar,T. (1998) Urinary and serum muatagenicity studies with rats implanted with depleted uranium or tantalum pellets. *Mutagenesis*, **13**, 101–106.
3. Miller,A.C., Whittaker,T., Hogan,J., McBride,S. and Benson,K. (1996) Oncogenes as biomarkers for low dose radiation-induced health effects. *Cancer Detect. Prev.*, **20**, 235–236.
4. Pellmar,T.C., Fuciarelli,A.F., Ejnik,J.W., Hamilton,M., Hogan,J., Strocko,S., Emond,C., Mottaz,H.M. and Landauer,M.R. (1999) Distribution of uranium in rats implanted with depleted uranium pellets. *Toxicol. Sci.*, **49**, 29–39.
5. Pellmar,T.C., Kaiser,D.O., Emond,C. and Hogan,J.B. (1999) Electrophysiological changes in hippocampal slices isolated from rats embedded with depleted uranium fragments. *Neurotoxicology*, **20**, 785–792.
6. Cugell,D.W., Morgan,W.K., Perkins,D.S.G. and Rubin,A. (1990) The respiratory effects of cobalt. *Arch. Intern. Med.*, **150**, 177–183.
7. Lauwerys,R. and Lison,D. (1994) Health risks associated with cobalt exposure—an overview. *Sci. Total Environ.*, **150**, 1–6.
8. Lison,D. and Lauwreys,R. (1995) The interaction of cobalt metal with different carbides and other mineral particles on mouse peritoneal macrophages. *Toxicol. In Vitro*, **9**, 341–347.
9. Lison,D., Carbonelle,P., Mollo,L., Lauwerys,R. and Fubini,B. (1995) Physiochemical mechanism of the interaction between cobalt metal and carbide particles to generate toxic activated oxygen species. *Chem. Res. Toxicol.*, **8**, 600–606.
10. Andrew,S.P., Caligiuri,R.D. and Eiselstein,L.E. (1991) A review of penetration mechanisms and dynamic properties of tungsten and depleted uranium penetrators. In Crowson,A. and Chen,E.S. (eds), *Tungsten and Tungsten Alloys: Recent Advances*. Plenum Press, New York, NY.
11. Patierno,S.R., Banh,D. and Landolph,J.R. (1988) Transformation of C3H/10T1/2 mouse embryo cells to focus formation and anchorage independence by insoluble lead chromate but not soluble calcium chromate: relationship to mutagenesis and internalization of lead chromate particles. *Cancer Res.*, **48**, 5280–5288.
12. Lin,X., Dowjat,K. and Costa,M. (1994) Nickel-induced transformation of human cells causes loss of the phosphorylation of the retinoblastoma protein. *Cancer Res.*, **54**, 2751–2754.
13 Lin,X. and Costa,M. (1994) Transformation of human osteoblasts to anchorage-independent growth by insoluble nickel particles. *Environ. Health Perspect.*, **102**, 289–290.
14. Rani,A.S., Qu,D., Sidhu,M.K., Panagakos,F., Shah,V., Klein,K.M., Brown,N., Pathak,S. and Kumar,S. (1993) Transformation of immortal, non-tumorigenic osteoblast-like human osteosarcoma cells to the tumorigenic phenotype by nickel sulfate. *Carcinogenesis*, **14**, 947–953.
15. Miura,T., Patierno,S.R., Sakuramoto,T. and Landolph,J.R. (1989) Morphological and neoplastic transformation of C3H/10T1/2 Cl 8 mouse embryo cells by insoluble carcinogenic nickel compounds. *Environ. Mol. Mutagen.*, **14**, 65–78.
16. Miller,A.C., Kariko,K., Myers,C.E., Clark,E.P. and Samid,D. (1993) Increased radioresistance of EJras-transformed human osteosarcoma cells and its modulation by lovastatin, an inhibitor of p21^{ras} isoprenylation. *Int. J. Cancer*, **53**, 302–307.
17. Rhim,J.S., Par,D.K., Arnstein,P., Huebner,R.J., Weisburger,F.K. and Nelson-Rees,W.A. (1975) Transformation of human cells in culture by N-methyl-N′-nitro-N-nitrosoguanidine. *Nature*, **256**, 751–753.
18. Reznikoff,C.A., Bertram,J.S., Brankow,D.W. and Heidelberger,C. (1973) Quantitative and qualitative studies of chemical transformation of cloned C3H mouse embryo cells sensitive to postconfluence inhibition of cell division. *Cancer Res.*, **33**, 3239–3249.
19. Landolph,J.R. (1985) Chemical transformation in C3H/10T1/2 Cl 8 mouse embryo fibroblasts: historical background, assessment of the transformation assay, and evolution and optimization of the transformation assay protocol. In Kakunaga,T. and Yamasaki,H. (eds), *Transformation Assay of Established Cell Lines, Mechanisms and Application*, IARC Scientific Publications no. 67. IARC, Lyon, pp. 185–198.
20. IARC/NCI/EPA Working Group (1985) Cellular and molecular mechanisms of cell transformation and standardization of transforming assays of established cell lines for the prediction of carcinogenic chemicals: overview and recommended protocols. *Cancer Res.*, **45**, 2395–2399.
21. Han,A. and Elkind,M. (1979) Transformation of mouse c3H/10T1/2 cells by single and fractionated doses of X-rays and fission-spectrum neutrons. *Cancer Res.*, **39**, 123–130.
22. Hill,C.K., Buonaguro,F.M., Myers,C.P., Han,A. and Elkind,M.M. (1982) Fission-spectrum neutrons at reduced dose rates enhance neoplastic transformation. *Nature (Lond.)*, **298**, 67–69.
23. Manara,M.C., Baldini,N., Serra,M., Lollini,P.L., De Giovanni,C., Vaccari,M., Argnani,A., Benini,S., Maurici,D., Picci,P. and Scotland,K. (2000) Reversal of malignant phenotype in human osteosarcoma cells transduced with the alkaline phosphatase gene. *Bone*, **26**, 215–220.
24. Perry,P. and Wolff,S. (1974) New giemsa method for differential staining of sister chromatids. *Nature (Lond.)*, **251**, 156–158.
25. Kohn,K.W., Erickson,L.C., Ewig,R.A.G. and and Friedman,C.A. (1976) Fractionation of DNA from mammalian cells by alkaline elution. *Biochemistry*, **15**, 4629–4637.
26. Anard,D., Kirsch-Volders,M., Elhajouji,A., Belpaeme,K. and Lison,D. (1997) *In vitro* cytotoxic effects of hard metal particles assessed by alkaline single cell gel and elution assays. *Carcinogenesis*, **18**, 177–184.
27. Barrett,J.C. (1993) Mechanisms of multistep carcinogenesis and carcinogen risk assessment. *Environ. Health Perspect.*, **100**, 9–20.
28. Romano,J.W., Ehrhart,J.C., Duthu,A., Kim,C.M., Appella,E. and May,P. (1989) Identification and characterization of a p53 gene mutation in a human osteosarcoma cell line. *Oncogene*, **4**, 1483–1488.
29. Rhim,J.S., Jin,S., Jung,M., Thraves,P.J., Kuettel,M.R., Webber,M.M. and Hokku,B. (1997) Malignant transformation of human prostate epithelial cells by N-nitroso-N-methylurea. *Cancer Res.*, **57**, 576–580.
30. Cooper,G.M. (1982) Cellular transforming genes. *Science*, **218**, 801–806.
31. Guerrero,I., Villasante,A., Corces,V. and Pellicer,A. (1984) Radiation-induced lymphoma in mouse. *Science*, **225**, 1159–1162.
32. Sawey,M.J., Hood,A.T., Burns,F.J. and Garte,S.J. (1987) Radiation-induced lymphoma in mouse. *Mol. Cell. Biol.*, **7**, 932–935.
33. Weinberg,R.A. (1991) Tumor suppressor genes. *Science*, **254**, 1138–1146.
34. Landolph,J.R. (1994) Molecular mechanisms of transformation of C3H/10T1/2 C18 mouse embryo cells and diploid human fibroblasts by carcinogenic metal compounds. *Environ., Health Perspect.*, **102**, 119–125.
35. Maehle,L., Metcalf,R.A., Ryberg,D., Bennett,W.P., Hariss,C.C. and Haugen,A. (1992). Altered p53 gene structure and expression in human epithelial cells after exposure to nickel. *Cancer Res.*, **52**, 218–221.
36. Lison,D. and Lauwerys,R. (1990) *In vitro* cytotoxic effects of cobalt-containing dusts on mouse peritoneal and rat alveolar macrophages. *Environ. Res.*, **52**, 187–198.
37. Lison,D. and Lauwerys,R. (1992) Study of the mechanism responsible for the elective toxicity of tungsten-carbide-cobalt powder toward macrophages. *Toxicol. Lett.*, **60**, 203–210.
38. Hatwig,A. (1995) Current aspects in metal genotoxicity. *Biometals*, **8**, 3–11.
39. Zelikoff,J.T., Li,J.H., Hartwig,A., Wang,X.W., Costa,M. and Rossman,T.G. (1988) Genetic toxicology of lead compounds. *Carcinogenesis*, **9**, 1727–1734.
40. Newman,S., Summitt,R.L. and Nunez,L.J. (1992) Incidence of nickel-induced sister chromatid exchange. *Mutat. Res.*, **101**, 67–75.
41. Sen,P. and Costa,M. (1985) Induction of chromosomal damage in Chinese hamster ovary cells by soluble and particulate nickel compounds: preferential fragmentation of the heterochromatic long arm of the X-chromosome by carcinogenic crystalline NiS particles. *Cancer Res.*, **45**, 2320–2325.
42. Costa,M., Salinkow,K., Cosentino,S., Klein,C.B., Huang,X. and Zhuang,Z. (1994) Molecular mechanisms of nickel carcinogenesis. *Environ. Health Perspect.*, **102**, 127–130.

43. Huang,X., Zhuang,Z., Frenkel,K., Klein,C.B. and Costa,M (1994) The role of nickel and nickel-mediated reacive oxygen species in the mechanism of nickel carcinogenesis. *Environ. Health Perspect.*, **102**, 281–284.
44. Touati,D. (2000) Iron and oxidative stress in bacteria. *Arch. Biochem. Biophys.*, **373**, 1–6.
45. Toyokuni,S. (1999) Iron-induced carcinogenesis: the role of redox regulation. *Free Radic. Biol. Med.*, **20**, 553–566.
46. Kitahara,J., Yamanaka,K., Kato,K., Lee,Y.W., Klein,C.B. and Costa,M. (1996) Mutagenicity of cobalt and reactive oxygen producers. *Mutat. Res.*, **370**, 133–140.
47. Cullen,M.R. (1984) Respiratory diseases from hard metal or cobalt exposure: a continuing enigma. *Chest*, **86**, 513–514.

Received April 14, 2000; revised September 6, 2000; accepted September 25, 2000